NEXTTRIP

INTERACTIONAL AERODYNAMIC ASSESSMENT OF AN ADVANCED TILT ROTOR CONFIGURATION

Evert Geurts, evert.geurts@nlr.nl, Netherlands Aerospace Centre NLR, the Netherlands
Gianni Bernini, gianni.bernini@leonardocompany.com, Leonardo Helicopters, United Kingdom
Andrea Battiston, a.battiston@hit09.com, HIT09, Italy
Rita Ponza, r.ponza@hit09.com, HIT09, Italy
Oliver Schneider, oliver.schneider@dlr.de, DLR, Germany

Abstract
This paper reports on the goals accomplished by the NEXTTRIP Consortium in response to the Topic JTI-CS2-2017-CFP06-FRC-01-15 titled "Interactional Aerodynamic Assessment of Advanced Tilt Rotor Configuration". The aim of the project was to assess different empennage configurations for the Next Generation Civil Tilt Rotor, NGCTR, by a large scale wind tunnel experiment, share knowledge and skills across the European partners and to provide guidance to the Integrated Technology Demonstrator (ITD) leaders through CFD-optimised and cost-effective solutions. The investigation, test and evaluation of a new empennage configuration for the NGCTR Technology Demonstrator were conducted in the DNW 9.5-by-9.5 m large low speed facility (LLF) in Marknesse, the Netherlands. Although the wind tunnel campaign was mainly focused to determine the stability and control characteristic of the powered, 1/5th scale model of the NGCTR, tests were also conducted to study the following effects of varying the basic configuration: effect of a V-tail and T-tail empennage, effect of elevator trim, effect of lateral-directional control, effect of power, interactional effect of rotor on/rotor off and effect of nacelle angle. Additional and innovative aspect of the experimental campaign was the application of the Particle Image Velocimetry based on Helium Filled Soap Bubbles, or HFSB, on large scale by using a seeding rake on 3-by-3 meters and up to 60 m/s. The test results were used in parallel to develop and validate a CFD methodology, based on multi-objective genetic algorithm, to optimise the V-tail empennage. Moreover, the project led to a fruitful exchange of ideas, expertise and knowledge, strengthening the bonds between JU partners.

1. INTRODUCTION

Within the CS2 FRC ITD Rotorcraft a Next Generation Civil Tilt Rotor Technology Demonstrator (NGCTR-TD) is being developed under leadership of Leonardo Helicopter Division. A key aspect of the design is to identify the optimal empennage configuration which needs to be effective in stabilizing and controlling the NGCTR in forward flight and the transition between hover and forward flight.
Due to location of the empennage and the tilting rotors, the area of the empennage has high aerodynamic interaction with the turbulent wake behind the rotors. Due to the nature of the complex airflow phenomena in that region, experimental tests with a powered wind tunnel model are required to adequately capture the flow phenomena in various flight conditions.

The main objective of the NEXTTRIP project was to assess and confirm the key choices on NGCTR-TD empennage configurations through wind tunnel tests and to provide guidance and proposals to the ITD leaders for further optimizing and improving the design on NGCTR.

For time- and cost effectiveness, and avoiding duplication of work, the NEXTTRIP project was built on knowledge, equipment and facilities generated in earlier research activities. More precisely, the knowledge and facilities (1:5 wind tunnel model) of the EU FP6 NICETRIP project were used, in which the NEXTTRIP consortium partners were actively involved and therefore have first-hand insight.

The main objective can be broken down into three sub-objectives

- Modify the existing 1:5 scale NICETRIP model to accommodate two new empennage geometries.
- Complete a powered (and non-powered) wind-tunnel campaign for a relevant test matrix that is based on NICETRIP experience and which captures the flow phenomena in relevant flight conditions in reports (forces, moments, pressure).
- Based on the processed wind tunnel data, define and execute a strategy with the aim to propose enhancements for the geometries, supported by CFD analysis.

Presented at 47th European Rotorcraft Forum, Glasgow, Scotland, 7-10 September, 2021

2. DESIGN AND MANUFACTURING OF THE POWERED MODEL

2.1. Baseline model

Within the EU FP6 programme NICETRIP a 1/5th scale full-span, powered wind tunnel model has been designed and manufactured by NLR and tested in DNW-LLF (see *Figure 1*) and ONERA S1, with support of DLR. In order to fully exploit the FP6 research program, the NEXTTRIP project is based on re-using the existing NICETRIP powered model and key-partners responsible for the successful execution of the NICETRIP low speed test.

Figure 1: NICETRIP full span powered wind tunnel model in DNW-LLF

The NEXTTRIP powered wind tunnel model parts, re-used from NICETRIP, have a central gearbox with two output drive shafts connected to a gearbox in each of the rotatable nacelles. Each prop rotor gearbox was attached to its own balance and the entire aircraft was mounted on a dedicated internal 6-component balance. The rotors are equipped with a swash-plate enabling collective and cyclic blade pitch settings to be made. Temperature sensors were used to continuously monitor the central and rotor gearbox operating conditions. The wing has two flaps and two flaperons that are remotely controlled. The hinge moments of all control surfaces are measured separately.

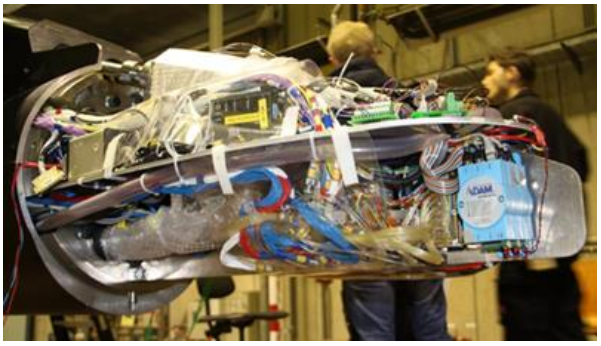

Figure 2: Equipment inside the model nose

The model was equipped with numerous static pressure ports and dynamic pressure transducers.

The majority of the on-board measurement system was situated in the detachable model nose (see *Figure 2*).

The major goal of the current NEXTTRIP programme, (acronym for NEXT generation civil Tilt Rotor Interactional aerodynamic tail oPtimisation), is to investigate the fundamental interactional aerodynamic aspects in the tail region of the tilt rotor aircraft and to get a clear understanding of the efficiency (in terms of aircraft static stability) of different empennage configurations when embedded in the rotor inflows.

2.2. T-tail and V-tail

In order to meet that goal the NICETRIP model (1:5) needed to be adapted to host the two proposed empennage configurations of the NGCTR configuration. These smaller tails (scale 1:3.8) consequently needed adjustment of the tail cone.

The T-tail consists of a horizontal tail plane, which has deflectable elevators, and a vertical tail which contains a deflectable rudder. An impression of the new T-tail assembly is presented in *Figure 3*.

Figure 3: New T-tail assembly

The V-tail consists of two surfaces mounted on a V-tail foot; the two V-tail surfaces have deflectable ruddervators. An impression of the new T-tail assembly is presented in *Figure 4*.

Both the T-tail and V-tail contain static pressure taps and dynamic pressure sensors.

All control surfaces have level plates to be used to determine the zero degree deflection. The rudder, elevator and ruddervators are deflected by means of remote controls and are equipped with hinge moment balances.

Presented at 47th European Rotorcraft Forum, United Kingdom, 7-9th September, 2021

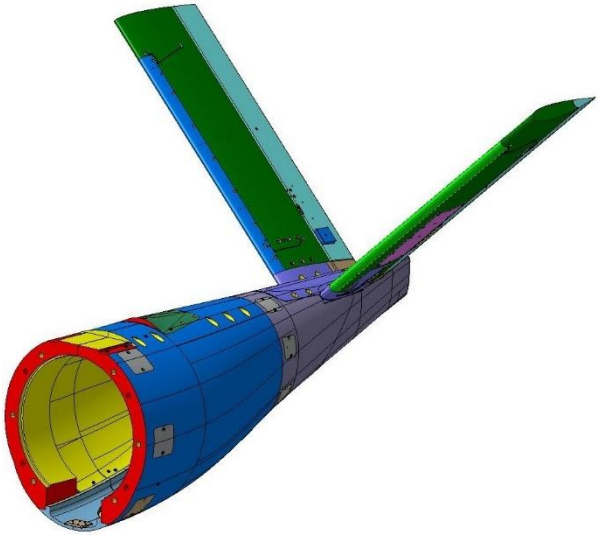

Figure 4: New V-tail assembly

The range of all control surfaces is summarized below (*Table 1*) as well as the positive directions of control surfaces and main bodies:

	Range	Remark
Elevator	±30˚	Trailing edge down = positive
Rudder	±30˚	Trailing edge right* = positive
Ruddervators	±30˚	Trailing edge down* = positive
Angle of Attack		Nose up = positive*
Angle of Sideslip		Nose to port (left) = positive*
Flap/Flaperon		Trailing edge down = positive
Nacelle	+0˚	Aircraft mode
Nacelle	+90˚	Helicopter/Hover mode
	*	(pilots view)

Table 1: Control surfaces and main body directions and ranges

2.3. Rear fuselage

The rear fuselage/tail cone was manufactured newly as the geometry differed from that of the NICETRIP project. The axial bolted connection with the rest of the fuselage is unchanged except for the fact that two additional bolt covers have been made. The additional bolt covers are required because the sponsons that covered the bolts during NICETRIP are not tested during NEXTTRIP. The rear fuselage houses the 6 component tail balance; the connection of fuselage/balance and balance/tail has remained the same. With similar loads acting on the tail, the tail balance was re-used.

2.4. Rotor and rotor blades

With the smaller tails the position and diameter of the rotors was not compatible to represent a realistic impingement of the rotor helix to the tails. With new rotor blades (see Figure 5), properly scaled in terms of diameter (40% larger) and disk loading, the high-gradient inflow characteristics are more representative of the flow field behaviour in the tail region of the Technology Demonstrator, bringing value and an overall benefit to the project.

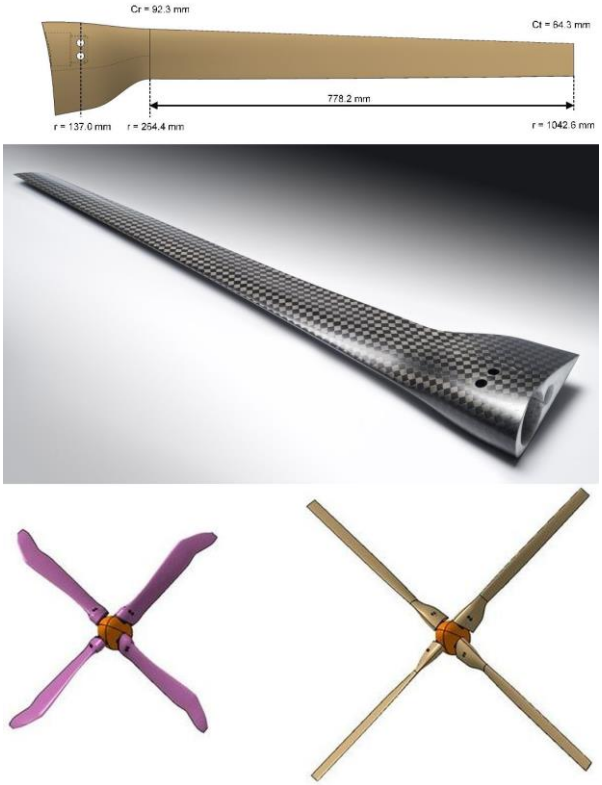

Figure 5: New rotor(blades)

The blade structure (foam core with fibre reinforced skin) needs to withstand the centrifugal loads due to the rotor speed and the aerodynamic loads (lift, drag, torsion) on the blade. The loads are transferred to the rotor shaft by steel attachment pins. As the NICETRIP rotor shaft is re-used, the interface between blade and shaft was fixed and remained unmodified.

For “Safety of Flight Monitoring” the rotor blades were instrumented with strain gauges to allow blade bending and torsional moments to be measured while temperature sensors

3. TEST PRAPARATIONS

3.1. Blades balancing

The new blades slightly differed individually and needed to be balanced. Balancing was only done in spanwise direction, not in chordwise direction because this was not measurable accurately enough. Because there is no method to balance the rotor head plus installed blades during the preparation phase at NLR it was decided to

Presented at 47th European Rotorcraft Forum, United Kingdom, 7-9th September, 2021

balance the rotor blades themselves. This was done in a static manner by determining the mass and the centre of gravity (CoG) of each blade. After this exercise, the blades (plus mounting pins) with mass and CoG closest to one another (taking into consideration LH and RH blades and at least 2 instrumented blades per rotor) were coupled, resulting in 4 sets of two blades plus 2 additional spare blades.

The two blades in each of the four sets of blades still have different static moments (CoG x mass), which needed to be corrected. Where required, additional masses were added in the foot of the blade. The same exercise was repeated till the ISO standard was met.

Finally, dynamic balancing to account for the weights to be added to the rotor head to remove the final unbalance, was performed. During spinning it was concluded that no unbalance was present and further balancing was not necessary.

3.2. Empennage balances

The overall tail loads of both T- and V-tail were measured with the existing NICETRIP tail balance, since the overall load range was adequate. It was decided not to perform a new calibration of the tail balance in case of a positive load verification check. In the preparation phase this seemed to be the case.

Since the new tails were different in shape and load range compared to the NICETRIP T-tail, the control surfaces of both tails were equipped with new hinge moment/torque balances (1-comp.); 3 for the T-tail (RH elevator, LH elevator, rudder) and 2 for the V-tail (LH and RH ruddervators). These balances all consist of an instrumented shaft with torsion strain gauges. The balances are located in the moment reference axes of each control surface.

All new balances were calibrated. Load monitoring equations were generated to be used online during wind tunnel testing to detect a possible overload. These equations were only to monitor stresses from a mechanical point of view. The initial calibrations were done at laboratory conditions with dedicated calibration cables and instrumentation. Load checks were performed in the wind tunnel before final use as the balances are part of a complete set of wiring and data acquisition equipment.

3.3. Model control and piloting

The NEXTTRIP model contains 16 built-in actuators. The actuator system is split into two parts. One part controls both swashplate systems

- 3 LH nacelle actuators and
- 3 RH nacelle actuators.

The second part controls all the other surface actuators

- LH and RH nacelle,
- LH and RH wing,
- LH and RH flaperon,
- LH and RH flap,
- Rudder, exchanged with RH ruddervator and
- Elevator, exchanges with LH ruddervator.

The surface control actuators are controlled with software implemented in the DLR piloting system.

The central part of DLR's operators display shows a static picture of the model (top view) and control boxes which are placed adjacent to the model part to control. It is possible to switch between the V-tail and T-tail configuration depending on the actual mounted configuration (see *Figure 6*).

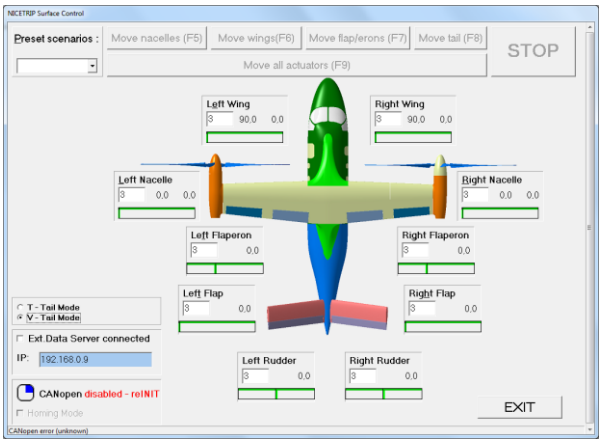

Figure 6: Surface actuator control program

In the control boxes, one can enter new setpoint values and tell the actuators to move by pressing the ENTER button. By pressing one of the function buttons (F5 to F9), the actuators will move in groups. The actual value is displayed in the boxes on the top right and the green bar at the bottom will visualize the position as well. Preset standard scenarios can be chosen from the list on the top left.

The system can be switched into "homing mode". In "homing mode" every actuator performs a pre-defined movement and stops at the "home switch" defining the special home position. This position is the reference for any movement.

The pilot uses a human machine interface to control both swashplate systems based on four control modes.

- Common: both swashplate systems react in the same way
- Differential: the RH swashplate reacts in a positive way, the LH one in a negative way.

Presented at 47th European Rotorcraft Forum, United Kingdom, 7-9th September, 2021

- RH: only the right hand swashplate can be controlled.
- LH: only the left hand swashplate can be controlled.

So the pilot can set the overall thrust by using the common mode. If there is remaining rolling or yawing moment, this can be compensated by using the differential mode. The overall thrust stays the same. The central knob (*Figure 7*) is used to set the collective angle, the left and right knobs are used to set the cyclic angles. The switch on the bottom right is used to set the control mode and the displays will show the calculated angles, based on the strokes of the actuators.

Figure 7: Pilots HMI interface for swashplate control

Concerning DLRs new data acquisition system for the models analogue sensors (moments, angles, forces) it was necessary to develop new data visualization software for the project (see *Figure 8*).

Figure 8: Main pilots display

New request and analysing methods were developed based on the pilots and customer requirements. Two new bargraph indicators were implemented to show the current trim of the rotors. The data processing concept based on the signal data base was still the same.

Beside database equation checks e.g. the correct equation for CT and the coefficients for forces and moments matrices the signal calculation from raw voltage to true physical values was accurately checked during preparation. Furthermore the offset calculation based on DLRs External Data Server data was realised. The new pilots display is able to perform the data acquisition request, data calculation and displaying the desired data information as the pilot it expects.

Other signal checking software was upgraded by DLR that show live measurement data used for calibration checks and for signal data quality examinations.

3.4. Sensor calibration and load checks

During the preparation phase, the model was mounted on the so-called 'Sting Dummy' in the experiment hall of DNW-LLF including the DNW main balance and drive system, providing the pressure to operate two air motors at nominal rotor RPM and thrust loads. All sensors of the model were connected to the DLR data acquisition system except pressure sensors which were measured by DNW.

Most of the sensor calibrations were performed by NLR in 2010 during model assembly of the NICETRIP model in the NLR workshop. One part of the preparation activities prior to the wind tunnel experiment, was to check each sensor of the model for functionality and calibration factors. The sensors of the new components (V-tail, T-tail, rotor blades) were checked as well. Some sensors needed to be re-calibrated (blade pitch angle, blade pitch loads and the blade bending moments).

In order to check a sensor calibration, the deviation of the measured sensor output w.r.t. the applied input must be calculated and evaluated. This was done for each sensor.

During preparations only simple rotor balance load checks could be made. Thus, the acquired results are of minor accuracy compared to the calibration in the NLR laboratory. It was found, that both rotor balances work according to the specifications with deviations compared to the originally calibration factors.

In addition to the static load checks a test was performed by rotation of each rotor by hand for different azimuth angles in HC mode. Turning the rotors without load, the influence of eccentricity from the drive system to the balance in-plane forces on moments was identified. Rotor torque and thrust are not affected for both balances.

During the model's sensor checks the signals of the complete measurement chain came out as expected. The deviations of the angle calibrations are low (less than 1%).

Partially higher deviations of the load calibrations were observed. Because of time restrictions it was decided to not recalibrate the deviating load sensors; the calibration checks were rated as sufficient for safe piloting during the campaign.

Presented at 47th European Rotorcraft Forum, United Kingdom, 7-9th September, 2021

3.5. Ground Vibration Tests

Purpose of the GVT was to determine the modal characteristics of the model in aircraft mode and helicopter mode in the 2 tail configurations i.e.

- Resonance frequencies and damping
- (reduced) Mode shapes
- Frequency response Functions

During wind tunnel testing some conversion mode settings were tested. However, the GVT only addressed aircraft mode and helicopter mode.

Since time was limited during test preparations the choice of the limited locations of the accelerometers and the visualization of the mode shapes was highly based on the very extensive GVT of the NICETRIP campaign (Ref.3).

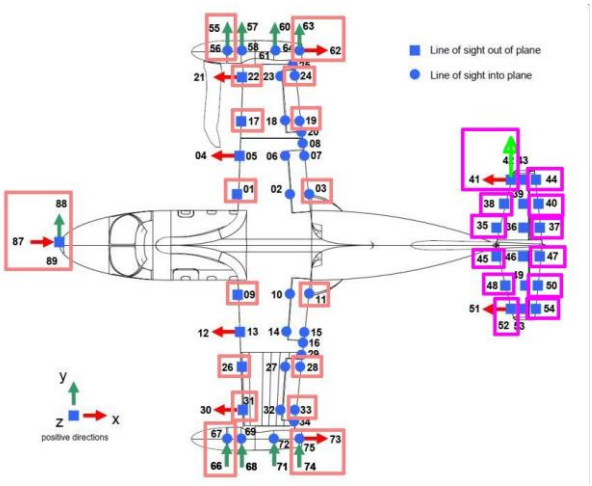

Figure 9: Representative selection of accelerometer locations in relation to NICETRIP GVT

With the above selection (*Figure 9*) various components were defined:

- Fuselage
- Nacelle – left/right – airplane/helicopter
- Outer wing – left/right – airplane/helicopter
- Inner wing – left/right
- T-tail – Horizontal Tail Plane – left/right
- T-tail – Vertical Tail Plane
- V-tail – left/right
- Blade3 – right

Proper grouping if the components allowed visualizing the 4 different geometries investigated: airplane mode T-tail, airplane mode V-tail, helicopter mode T-tail and helicopter mode for the V-tail configuration (see *Figure 10*).

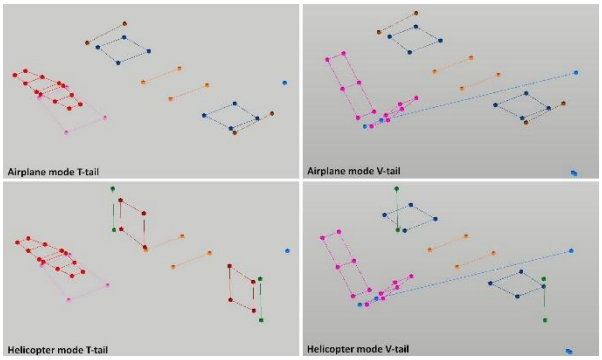

Figure 10: Geometry components ordered per GVT conf.

To get a quick overview of the frequencies present in the various configurations the structure is excited with random excitation. That is done for various exciter configurations at various locations. In order to fine-tune the frequencies normally swept sine excitation is used with different energy levels to investigate non-linearity. This was tried, but didn't bring the expected results. Since the tunnel slot was pinned and not much time was left to investigate the problem it was decided to finish at least all configurations with random excitation. Therefore the processing might be less accurate.

However, from NICETRIP GVT results, it was concluded that a high amount of damping was in the structure, which was expected not to change for the NEXTTRIP model. Although the energy levels for random excitation generally are low, and thus less indicative in comparison to swept-sine excitation, various excitation levels were applied. In spite of the low levels, it was observed that the structure behaved highly non-linear and highly damped. The damping is expected to increase further during rotation. Also wind-on is expected to have a beneficial contribution.

In the rotor blade design report an assessment was made of the natural frequencies of the new rotor blades it was concluded that there is a low risk that any of the natural frequencies of the blade coincides with any of the engine orders. Therefore, it is believed that the current design of the NEXTTRIP blade is adequate.

The above conclusion was based on a maximum RPM of 2029. Since Leonardo had a request for higher RPM beyond the original scope of the design above conclusion might become invalid.

Since a GVT on the blades only in advance to the preparations had not been performed, it was decided to perform an extra GVT on one of the spares of the new rotor blades. Since the boundary conditions are always a subject of discussion it was decided to apply the least debatable suspension, a free-free suspension by hanging the blade on bungee cords.

Presented at 47th European Rotorcraft Forum, United Kingdom, 7-9th September, 2021

Although based on results of the free-free suspension, the comparison justifies the conclusion that the modelling of the blades is a good representation of the reality, also for clamped conditions. Hence the accuracy of the Campbell diagram can be judged as realistic. Therefore, during testing, special attention should be paid to a possible excitation of the blades in second bending at the 4P blade passage.

4. WIND TUNNEL TEST

4.1. Overall measurements

The wind tunnel tests have been carried out at the subsonic 9.5 x 9.5 m test section of the DNW-LLF. The actual test period in the wind tunnel was split in two separate wind tunnel entries due to unforeseen circumstances (collapse of one anti-turbulence screen):

1. From 03 June 2019 to 19 June 2019

2. From 28 November 2019 to 10 December 2019.

During the second entry, additional tests were carried out without the tail units (no-tail configuration) to compensate for the lack of reliable tail balance measurements and cast some light on the tails behaviour.

The experimental program primarily covers the low speed range of the flight envelope, from helicopter mode through conversion to aircraft mode. Parametric variation of model component settings are made, such as: “fuselage” incidence and side-slip, outer wing and nacelle tilt angles, control surface settings and rotor operating points. The test program concentrated on the following subjects:

- Aerodynamic interactions
- Tail effectiveness: V-tail and T-tail
- Evaluation of
  - ✓ Applicability of Heyson wall correction method for tilt rotors (see Ref. 4)
  - ✓ Development of helium filled soap bubbles PIV measurement technique for industrial application

Additional to the instrumentation mentioned in section 2.1, the model contained 684 static pressure taps and with 54 dynamic pressure sensors (Kulite), all at the starboard side of the model

The test matrix consisted of hover, conversion and low-speed forward flight conditions. Seven trim points were defined depending on wind tunnel speed and nacelle angle:

- 2 helicopter conditions (HC)
  with constant nacelle angle at 90º:
  HC2: V=15.4 m/s, and
  HC3: V=29.6 m/s
- 4 conversion conditions (CC)
  at various nacelle angles and wind speed:
  CC1: V=22.9 m/s, nacelle at 75º,
  CC2: V=37.0 m/s, nacelle at 75º,
  CC3: V=40.7 m/s, nacelle at 50º, and
  CC4: V=44.4 m/s, nacelle at 30º.
- 1 aircraft condition (AC)
  with constant nacelle angle at 0º:
  AC1: V=60 m/s.

During the NICETRIP tests in 2013 a damage of all rotor blade bearings took place due to high loads while using cyclic pitch control and it was decided to omit cyclic pitch inputs. In the NEXTTRIP tests this was done as well to reduce loads on the blade bearings and prevent bearing damages. During model trimming cyclic pitch angles were adjusted to zero. This leads to high in-plane moments at the rotors.

Trim goal was the thrust coefficient c_T, which was controlled using the collective blade pitch. Before starting the test matrix measurements for a test condition the maximum allowable wind speed and rotor rpm was determined by monitoring the rotor in-plane and 1/rev shaft bending moments. In some cases it was necessary to reduce rotor rpm and wind speed in order to keep a constant advance ratio. No use of cyclic pitch led to limitations in rotor speed and wind tunnel speed (see *Figure 11*) due to high loads on the rotor balances and shafts.

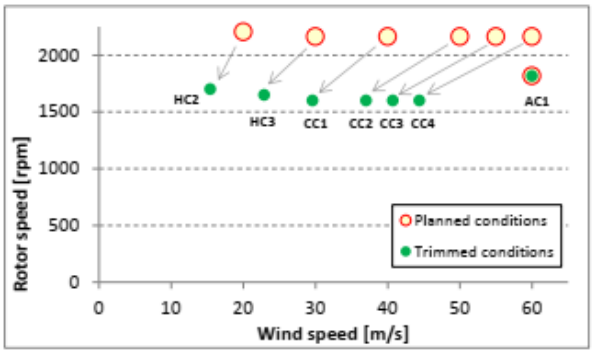

Figure 11: Planned and trimmed test conditions

Since the test campaign suffered from the anti-turbulence screen drop, it was possible to post-process results from the first entry. From this processing tail balance data were interpreted as not reliable. Therefore, after the first wind tunnel entry, but before the second entry, NLR conducted additional analyses concerning the tail balance, but no conclusion could be drawn. Since the outcome of the intermediate tests was unknown to be adequate for reliable tail balance data, as an extra mitigation action the test program for test entry 2 was adapted.

Presented at 47th European Rotorcraft Forum, United Kingdom, 7-9th September, 2021

In test 1 only the V-tail configuration could be measured. In test 2 the T-tail test were conducted completely. To have some direct comparison measurements the HC2, HC3 and AC1 condition were repeated in test 2 and additionally tests without a tail were performed as well. An overview of all conditions tested is listed in Figure 12 separated in test 1 and 2.

	Rotor Off			Rotor On		
	V-tail	T-tail	No-tail	V-tail	T-tail	No-tail
HC2	T2			T1, T2	T2	T2
HC3	T1, T2	T2		T1, T2	T2	T2
CC1				T1	T2	T2
CC2	T1	T2		T1	T2	T2
CC3	T1	T2		T1	T2	T2
CC4				T1	T2	T2
AC1	T1, T2		T2	T1, T2	T2	T2

Figure 12: Condensed test matrix

One of the configurations tested was the model with V-tail in helicopter mode, which is depicted in *Figure 13*.

Figure 13: V-tail configuration in helicopter mode in LLF

4.2. Flow visualization

The impact assessment of the rotor wakes on the empennage efficiency and loads are not only investigated by means of local load and pressure measurements but also with advanced flow visualization

One of the ambition, beyond the state of the art, for this project was to mature the HFSB technique for application in large industrial wind tunnels, providing an excellent flow visualisation enabling better understanding of the interactional flow phenomena from rotor to empennage.

The Helium Filled Soap Bubble (HFSB) test technique is a technique based on the Particle Image Velocimetry (PIV) measurements, requiring seeding particles and a laser. A so-called seeding rake is used to generate small soap bubbles filled with Helium. The soap bubble is filled with Helium to compensate the weight of the soap and to a limited extend the inertia of the soap bubble. The helium filled soap bubble is generated by a nozzle. The nozzle is designed and manufactured by NLR. The rake contains 400 nozzles distributed in an array of 20 by 20 nozzles. The rake has a width and height of 3 by 3 meters.

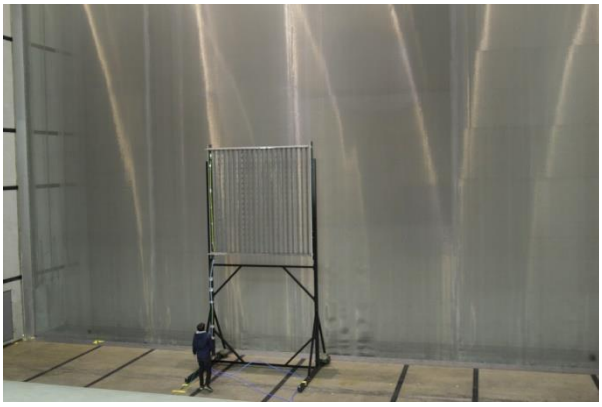

Figure 14: HFSB-rake in LLF settling chamber

The HFSB-rake is mounted on a frame in the settling chamber of the DNW-LLF, see *Figure 14*. Since this is a try-out for industrial testing it was decided, in order to minimize costs, to fix the HFSB-rake on a frame instead of developing a traversing system. Due to load limitations the frame height for the HFSB-rake is limited. This implies the seeded stream tube is fixed in the wind tunnel. Hence the model position is altered to move the region of interest around the model into the stream tube that is seeded with the HFSB.

The laser sheet is fixed to the wind tunnel. The model is moved up and down to vary scan plane with respect to the model. It is evident that moving the model in closer proximity to the wind tunnel floor affects the position of the wake with respect to the model mainly due to wall interference. These effects are expected to be more significant the closer the model gets to the wind tunnel floor.

Figure 15:HFSB seeding for PIV

Figure 15 shows the laser light sheet illuminating the HFSB seeding in a stream tube of 1m x 1m (due to contraction) on the port side of the model.

Presented at 47th European Rotorcraft Forum, United Kingdom, 7-9th September, 2021

5. DATA ANALYSIS

5.1. OVERVIEW

The tests described here were undertaken primarily to investigate the stability behaviour of both the T-tail and V-tail design and their interactions with the rotors' wake at different conditions of angle of attack, angle of sideslip, rotors power, nacelle angle and free stream velocity. Particular attention was paid to investigate the impact of the rotors wake on the tail region in conditions of low speed and moderate to high sideslip angles and its effect on the airframe pitching moment. The model was equipped with a main balance and a dedicated tail balance but only the main balance's forces and moments were used to assess the behaviour of the tails and, in general, of the entire aircraft as the tail balance data were deemed unreliable due to the presence of an unrepairable drift. All the quantities displayed in the following plots are forces and moments of the airframe only, i.e., the total integral quantities minus the forces and moments of the two rotors. This was done to highlight the interactional effects of the spinning rotors on the airframe of the aircraft.

Apart from the test's application to the NEXTTRIP wind tunnel model, the results in terms of trends can be applied to other aircraft of similar layout.

5.2. EXPERIMENTAL DETAIL

The model represented a combination of the ERICA tiltrotor main body with the addition of two new tail units derived from the AW609 technology demonstrator (TD). This hybrid configuration is referred in this document as the NEXTTRIP model. A new set of rotor blades having a radius of 1.04m was also manufactured with the aim to reproduce the proportion between the wake stream tube and the position of the empennage of the NGCTR-TD. Boundary layer transition was fixed on the wings, fuselage, tailplane, vertical fin and on the two surfaces of the V-tail throughout the test by means of trip dots also referred to as cad-cut dots. The intake shape was correctly represented but there was no flow through the nacelles. The two tail units consisted of a conventional T-tail design and a V-tail concept mounted on a common support on the rear of the aircraft and sharing the same tailcone geometry. At the bottom of the aircraft, the interactional effect of the supporting sting was not taken into account because of the intention to compare the two tail designs by deltas rather than absolute quantities.

5.3. RESULTS

The results have been analysed to obtain indications on the directional and longitudinal stability characteristics of the conventional T-tail compared to the new V-tail concept. It has to be noted that the level of maturity of the V-tail design is such that it gives useful information about the general trends and characteristics and on the applicability of a V-tail solution to a tiltrotor aircraft. For a quantitative, direct, comparison with the T-tail, more work is needed to further refine the V-tail aerodynamic design and reduce the static deltas between the two units.

Longitudinal Stability

Measurements of lift coefficient, drag coefficient and pitching moment coefficient were made at Mach numbers from 0.044 to 0.176 on the basic aircraft model, with and without the tail unit. *Figure 16* and *Figure 17* show the variation of CL, CD and CM with α for each condition ranging from edgewise flight (nacelle 90 degrees) to conversion corridor to airplane mode (nacelle angle 0 degrees). The variation of lift and drag with both incidence and Mach followed a similar pattern for each of the two tail configurations. For the V-tail the variation of the pitching moment with incidence up to 25 degrees show a constant slope with a plateau in the range of 5° < α < 10° for the nacelle 90 degrees Mach 0.044 condition. The T-tail design shows a larger incidence range where the pitching moment is almost constant with an unstable slope observed between 5 < α < 15 for the nacelle 90° (Mach 0.044) and nacelle 75° (Mach 0.066).

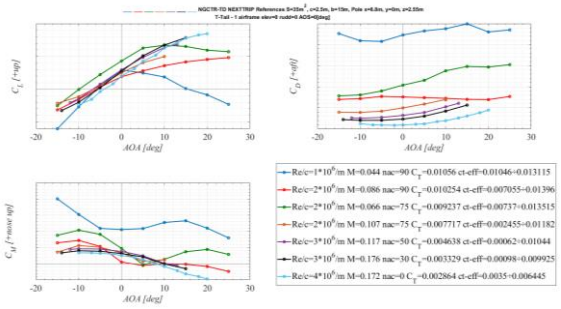

Figure 16: V-tail aerodynamic characteristics at different Mach numbers and nacelle angles

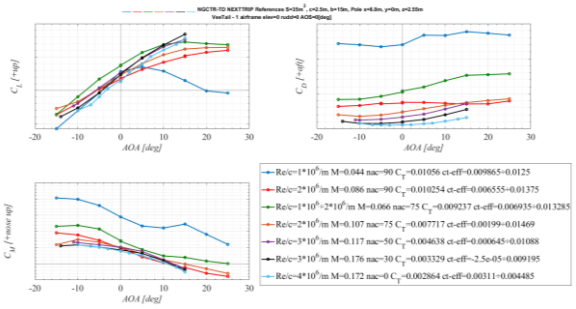

Figure 17:-T tail aerodynamic characteristics at different Mach numbers and nacelle angles

Presented at 47th European Rotorcraft Forum, United Kingdom, 7-9th September, 2021

The interactional effect of the rotors decreases the CL slope compared to the rotor off case, increases the drag coefficient considerably especially at incidences around 0° but has a limited effect on the pitching moment characteristics at positive angles of attack. The data with the aircraft equipped with the conventional T-tail design show an increased CL slope for the rotor off case but a negligible benefit during rotor on conditions. The longitudinal stability does improve with the T-tail unit mounted compared to the no-tail configuration but this improvement is considerably reduced in rotor on conditions with a large CM plateau region between 0° < α < 15°.

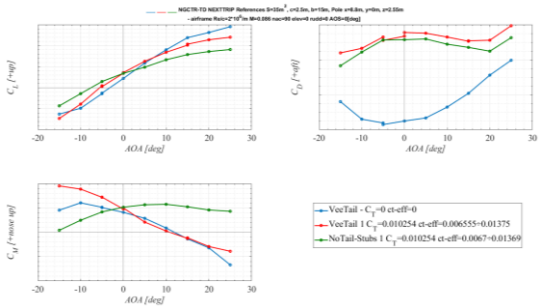

Figure 18: V-tail effect on the airframe aerodynamic characteristics and interactional effect of the rotors

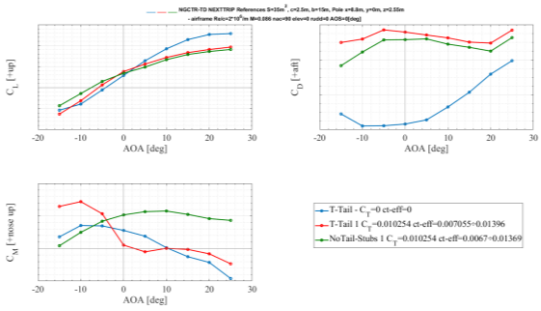

Figure 19: T-tail effect on the airframe aerodynamic characteristics and interactional effect of the rotors

Directional Stability

The NEXTTRIP model was tested at different yaw angles up to 26.5° at Mach numbers between 0.044 and 0.176. The purpose of high yaw testing was to measure the direct impact of the rotor wake on the tail units and assess the directional stability characteristics of the airframe as well as the effect of the sideslip on the pitching moment of the aircraft. Along with a tail-off configuration, both T-tail and V-tail empennages were tested. *Figure 20* and *Figure 21* show the variation of yawing-moment coefficient CN with the sideslip angle for the 'no tail' configuration and the 'tail on' configurations at rotor on and rotor off conditions. The installation of the tail units improves the directional stability of the aircraft although the rotor wake in the power on condition at a nacelle angle of 90° has the effect of turning the CN slope from positive (stable) to negative (unstable). This behaviour has been observed for both the V-tail and T-tail designs. By looking at the pitching moment coefficient, despite some differences between the T-tail and V-tail in terms of absolute values, the trends are very similar. In rotor on conditions (red line) the pitching moment increases steadily as β increases. For rotor off condition the CM shows a slightly negative slope, once again highlighting the substantial effect of the interaction of the rotor wake with the tail region of the aircraft. The installation of the empennages in rotor on conditions increases the rolling moment and a similar behaviour between the T-tail and V-tail is observed. During rotor off testing, instead, the two tail units produced a different effect with the V-tail showing a similar slope compared to the rotor on condition up to 15 degrees and then a plateau at higher β. The T tail effect at C_T=0 is equivalent to the no tail rotor on condition in terms of rolling moment.

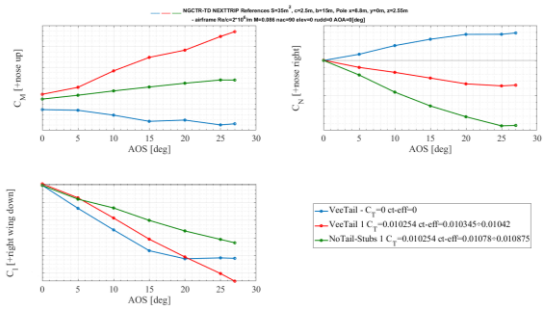

Figure 20: V-tail intallation and interactional effects on the airframe pitching moment, yawing moment and rolling moment with sideslip

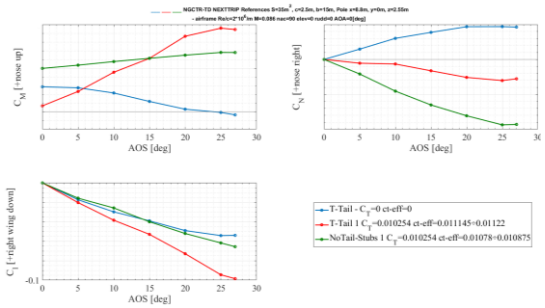

Figure 21: T-tail installation and interactional effects on the airframe pitching moment, yawing moment and rolling moment with sideslip

Representative curves of the variation of sideforce, yawing moment and rolling moment with β at various Mach numbers / nacelle angles is given in *Figure 22* and *Figure 23*. It will be seen that there

Presented at 47th European Rotorcraft Forum, United Kingdom, 7-9th September, 2021

is a moderate directional stability of the model with the tail unit on at high Mach numbers and low nacelle incidence angles. At Mach 0.107 and nacelle at 75 degrees a neutral stability is observed. Starting from Mach 0.086 and below there is a region of instability. The instability persists to the lowest Mach numbers and pure edgewise flight condition. The rate of change of side force with β is similar across the range of Mach numbers tested with a shared behaviour between the V-tail and the T-tail empennage. Variation of dCl/dβ with Mach number are also presented and once again the V-tail and T-tail show a similar behaviour. For all the conditions tested but the one at the lowest Mach number, an increase in sideslip (nose to left) results into a negative rolling moment (left wing down). The effect is less pronounced at high Mach numbers and low nacelle angles. The edgewise flight condition at Mach 0.044 is the only one to show a positive rolling moment with increasing sideslip.

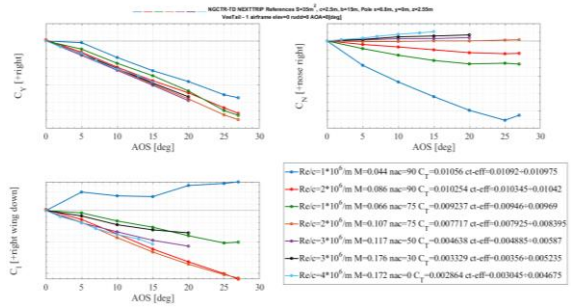

Figure 22: V-tail sideforce, yawing moment and rolling moment for different Mach numbers and nacelle angles

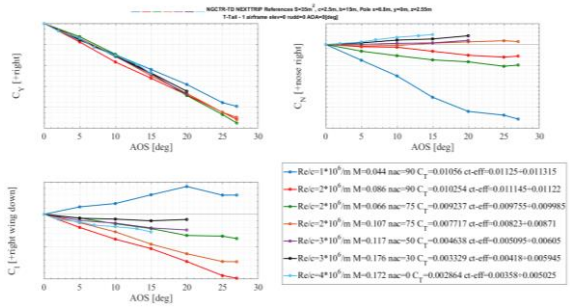

Figure 23: T-tail sideforce, yawing moment and rolling moment for different Mach numbers and nacelle angles

6. NGCTR EMPENNAGE OPTIMIZATION

The present section aims at describing the overall optimization strategy implemented for enhancing the aerodynamic performance of the NGCTR empennage surfaces. Based on given specification – regarding: (a) the reference case geometry; (b) the reference test conditions; (c) the main aerodynamic requirements of the NGCTR; (d) the targets for aerodynamic performance enhancement with respect to the baseline geometry; (e) the tail unit structural and geometrical constraints of the NGCTR – a sequential approach for the design optimization was followed. The procedure was made up of the following main steps: (1) Optimization of the V-tail empennage airfoil using a 2-dimensional CFD model, with the aim of minimizing drag and hinge moment coefficients; (2) Optimization of the tail winglets – patented under Leonardo Helicopters under the name of Finlets - using a 3-dimensional CFD model, with the aim of increasing the V-tail longitudinal and latero-directional stability, while at the same time minimizing drag and lowering rolling moment at the tail root.

The empennage baseline geometry, which was the subject of optimization, is depicted in Figure 24.

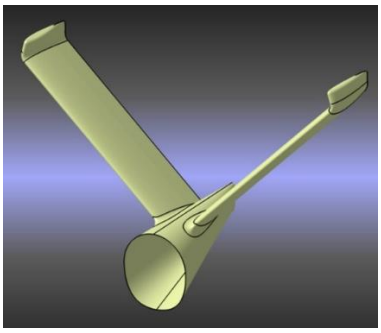

Figure 24. Empennage baseline geometry.

6.1. AIRFOIL 2D OPTIMIZATION

The 2D airfoil optimization objectives were: (1) minimization of the drag coefficient at cruise conditions; (2) maximization of control effectiveness at cruise and aircraft's near-stall conditions; (3) minimization of the hinge moment coefficient at cruise and near-stall conditions; (4) minimization of the hinge moment coefficient derivative with reference to the RVTR deflection angle at cruise and aircraft's near-stall conditions.
The constraints on the optimization were of both geometrical and functional nature: (1) symmetric airfoil; (2) straight upper and lower sides of the moving surface; (3) constraints on the lift coefficient derivative with respect to the angle of attack at cruise and near-stall conditions.

The optimization problem was formalized as a multi-objective multi-constrained problem in which the objectives were merged into a weighted sum fitness function, and the functional constraints were treated as a weighted sum of penalty functions. Such method made it possible to maintain the

Presented at 47th European Rotorcraft Forum, United Kingdom, 7-9th September, 2021

problem formally unconstrained, but at the same time to quantify the degree of violation of the functional constraints.

The fitness functions were written in form of minimization problem.

Three sets of optimizations were conducted at different RVTR deflection angle, with the aid of GeDEA-II (Refs 5 to 11), a proprietary evolutionary algorithm that treats the genetic diversity as an objective, thus emphasizing both the non-dominated individuals and the most genetically different ones, thus ensuring a wide exploration of the design space.

The results are summarized in the objectives space plots of Figure 25, where the Pareto Front for each RVTR deflection angle is illustrated. For each case, near-B Pareto individuals tend to respect all the constraints, while near-A individuals feature a higher increase in performance.

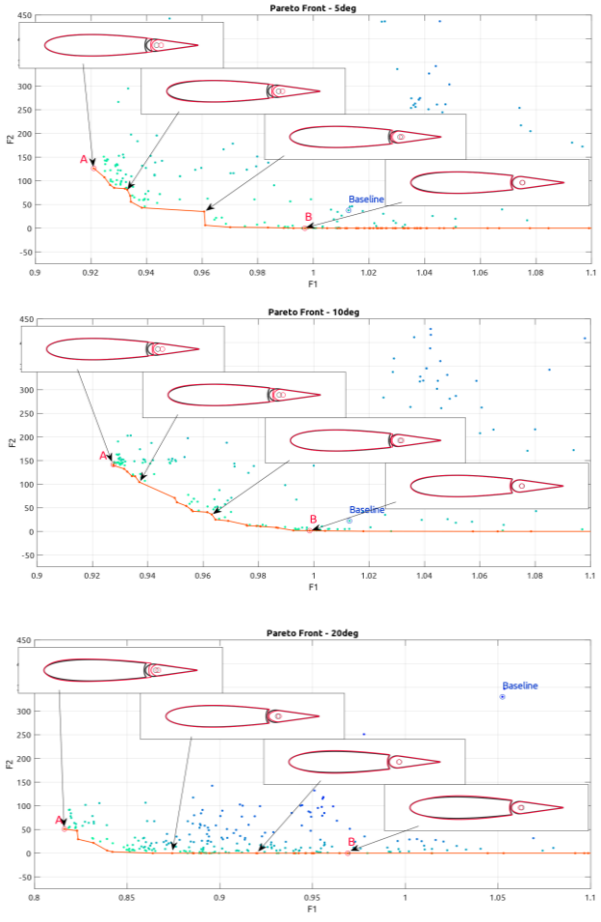

Figure 25. 2D airfoil optimization results.

From the three optimizations at different RVTR deflection angles, the individual B of the 10deg optimization was chosen as a tradeoff solution by Leonardo Helicopters. The improvement in aerodynamic performance of this shape with respect to the baseline is summarized in Table 2.

Coefficient	*Ind. B 10º*
CD (cruise)	-0.20%
CH (cruise)	0.04%
CLa (cruise)	-0.94%
CLde (cruise)	4.08%
CHde (cruise)	1.12%
CH (stall)	-1.49%
CLa (stall)	0.81%
CLde (stall)	0.67%
CHde (stall)	-4.09%

Table 2: Airfoil Optimization Results, expressed as percentage difference wrt the baseline.

It is apparent that the solution cannot simultaneously satisfy all the objectives and constraints. This was actually the case with all the individuals of the Pareto fronts, and it was caused by the fact that the problem was very highly constrained and characterized by the definition of a strong set of targets. Regarding the selected optimal individual, enhancements were observed for the drag coefficient in cruise conditions (-0.20%). The hinge moment showed a slight decrease in performance at cruise conditions (+0.04%), but at the same time, a significant improvement was observed at near-stall conditions (-1.49%). The derivatives of the lift coefficient both in cruise and near-stall conditions feature an improvement (+4.08% and +0.67% respectively). The lift coefficient derivative against the angle of attack is within the ±5% range of acceptability (-0.94% in cruise conditions and +0.81% in near-stall conditions).

6.2. FINLET 3D OPTIMIZATION

The Finlet optimization process was focused on two primary objectives: (1) minimization of the drag coefficient in cruise conditions; (2) minimization of the rolling moment at the tail root both in cruise and near-stall conditions. The functional constraints to the problem were: (1) the pitching moment derivative in near-stall conditions was requested to be the same of the baseline; (2) the yawing moment derivative both in cruise and near-stall conditions was bounded at ±5% range of variability with reference to the baseline values.

Similarly to the 2D optimization, the objectives were merged into a weighted sum fitness function. Also, the constraints, written as penalty functions, were treated as a second weighted sum.

A Design of Experiments was conducted prior to the optimization, with the aim of determine the influence of the Finlet geometrical features on the

Presented at 47th European Rotorcraft Forum, United Kingdom, 7-9th September, 2021

target aerodynamic coefficients. This was done in order to understand whether some design variables could be fixed, thus reducing the optimization computational effort.

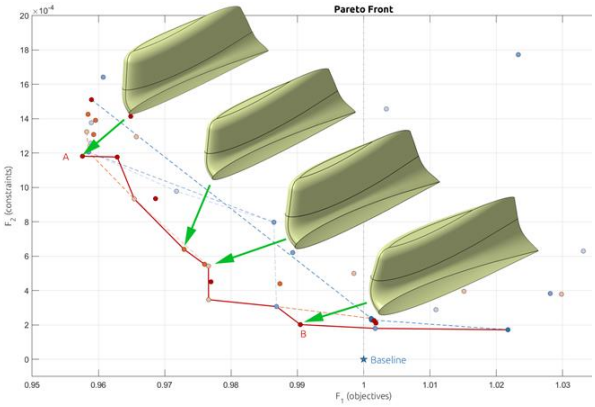

Figure 26. 3D Finlet optimization results.

The optimization was carried out, as previously, using GeDEA-II. The results, summarized in *Table 3*, are presented in a similar way of the aerofoil ones: the near-A individuals feature a higher improvement in aerodynamic performance, while the near-B individuals are more likely to respect the functional constraints, at the price of a lower aerodynamic performance (see *Table 3*).

Coefficient	*Ind. A*	*Ind. B*
CD (cruise)	-0.79%	-0.26%
CR (cruise)	-6.85%	-1.96%
CR (stall)	-4.42%	-1.57%
CMa (stall)	3.94%	2.48%
CNb (cruise)	-8.25%	-0.79%
CNb (stall)	-8.38%	-2.63%

Table 3: Finlet Optimization Results, expressed as percentage difference wrt the baseline.

It is worth noting that the aerodynamic coefficients (drag and rolling moment) of all the individuals in the Pareto Front (from A to B), are enhanced with respect to the correspondent baseline values.

Considering the two extremal individuals, meaningful enhancements are featured by individual A, which showed a decrease in drag coefficient of 0.79% with reference to the baseline, whilst individual B had an improvement of -0.26% on such coefficient. Regarding the rolling moment coefficient improvement, individual A featured a -6.84% (cruise conditions) and a -4.42% (near-stall conditions) reduction of the rolling moment, while at the same time individual B showed a smaller improvement on such coefficient (-1.96% in cruise conditions and -1.57% in near-stall conditions).

In terms of constraints, although individual A featured the best improvements in the objectives coefficients (drag and rolling moment), the yawing moment derivative showed a -8.24% reduction for cruise conditions and a -8.37% in near-stall conditions, whilst individual B maintained the correspondent values within the ±5% range (respectively -0.78% and -2.63%).

In terms of pitching moment derivative in stall conditions, the constraint was set as an equality function, therefore for both the individuals there is a certain degree of violation on such constraints (+3.94% for individual A and +2.47% for individual B).

The degree of constraints violation is more prominent while going towards individual A, although the near-A individuals featured better improvements in terms of objectives.

7. CONCLUSIONS

Special efforts were devoted at modifying the existing NICETRIP wind tunnel model in order to derive useful information for the NGCTR technology demonstrator (TD) with highly optimised and cost-effective solutions. A new T-tail, V-tail and composites rotor blades were manufactured and installed in what has become the NEXTTRIP wind tunnel model. Ad-hoc software modifications were made to the model control and piloting suite to reflect the modifications and updates introduced in NEXTTRIP. All moving parts were remote controlled during the test so configuration changes did have a minimum impact on the test's elapsed time. After a careful and intense test preparation phase to ensure full model functionality and safety, interactional wind tunnel tests with spinning rotors were conducted up to 60 m/s at the DNW LLF facility for a wide range of advance ratio, nacelle angle, rotor thrust, and control surface position combinations. The V-tail and T-tail installations were analysed and compared in terms of control power and stability. Similar aerodynamic characteristics were observed for the two tail designs apart from the pitching moment in the range $0°<\alpha<10°$ where the V-tail keeps a stable derivative whereas the T-tail shows a plateau of neutral stability. The rotor interactional effect on the airframe with the nacelle perpendicular to the wing and at Mach 0.086 results in a decrease of the lift derivative and an increase of drag. Moreover, for the same flight condition, the rotor-on cases change the airframe CM slope from negative to positive as well as the yawing moment direction from nose-to-right to nose-to-left. Finally, no abrupt pitching moment

Presented at 47th European Rotorcraft Forum, United Kingdom, 7-9th September, 2021

divergence has been observed with increasing sideslip either for the T-tail or V-tail empennage. As an element of innovation beyond the state of the art, helium filled soap bubble (HFSB) PIV tests were conducted successfully from a 3m by 3m seeding rake up to 60 m/s, showing the potential of this technique also for large scale industrial applications. With the aim to further enhance the performance of the NGCTR-TD, a dedicated tail aerofoil and Finlet optimisation was carried out by means of an evolutionary genetic algorithm based on multi-objective and multi-constrained problem. The highly constrained nature of the exercise led to the impossibility to satisfy simultaneously all the objectives and constraints but some improvement have been achieved. On the 2D aerofoil optimisation, reduction of drag, hinge moment and improvement of the lift derivatives were achieved. The Finlet optimisation let to the enhancement in the drag and rolling moment coefficients for individual B at the cost of a yawing moment derivative reduction.

8. SYMBOLS AND ABBREVIATIONS

a	Speed of sound	[m/s]
ALPHA, α	Angle of incidence, positive nose-up	[°]
BETA, β	Angle of sideslip, positive nose-to-left	[°]
CD	Drag coefficient	[-]
CL	Lift coefficient	[-]
CM	Pitching moment coefficient, positive nose-up	[-]
CY	Side force coefficient, positive right	[-]
CN	Yawing moment coefficient, positive nose-to-right	[-]
Cl	Rolling moment coefficient, positive right-wing-down	[-]
CT	Thrust coefficient of the rotor	[-]
HFSB	Helium Filled Soap Bubbles	[-]
MACH, Ma	Nominal Mach number	[-]
REYNOLDS, Re	Nominal Reynolds number	[-]
NAC	Nacelle angle, 90° in hover and 0° in airplane mode	[°]
NGCTR	Next Generation Civil Tilt Rotor	
TD	Technology Demonstrator	
PIV	Particle Image Velocimetry	
RVTR	Ruddervator	

9. REFERENCES

1. O. Schneider, NEXTTRIP: Test Report – contribution DLR, FRC–IADP–785350–NEXTTRIP–DNW D3.5 (Part2)
2. I. Philipsen, NEXTTRIP: Test report on measurements on the NEXTTRIP large-scale powered model in DNW-LLF, FRC–IADP–785350–NEXTTRIP–DNW D3.5
3. Govers, Y., "*Ground Vibration Test NICETRIP-2*", NICETRIP_WP34_D32_DLR_GOE
4. Iwan Philipsen, "Lift Interference Effects Evaluation for Powered Models in Closed-wall Low Speed Wind Tunnels", AIAA SciTech Forum 2021
5. Toffolo A., Benini E., "Genetic Diversity as an Objective in Evolutionary Algorithms", Evolutionary Computation, Vol. 11, No. 2, Summer 2003, pp. 151–167, doi: 10.1162/106365603766646816
6. Benini E., Comis da Ronco C., "GeDEA-II: A Simplex Crossover Based Evolutionary Algorithm Including the Genetic Diversity as Objective" Applied Soft Computing, Vol. 13, No. 4, April 2013, pp. 2104-2123. doi: 10.1016/j.asoc.2012.11.003
7. Toffolo A., Benini E., "A New Pareto-Like Evaluation Method for Finding Multiple Global Optima in Evolutionary Algorithms", Late Breaking Papers at the 2000 Genetic and Evolutionary Computation Conference, Las Vegas, NV, July 2000, pp. 405-410
8. Comis da Ronco C., Ponza R., Benini E., "Aerodynamic Shape Optimization of Aircraft Components Using an Advanced Multi-Objective Evolutionary Approach", Computer Methods in Applied Mechanics and Engineering, Vol. 285, 1 march 2015, pp. 255–290, doi: 10.1016/j.cma.2014.10.024
9. Comis da Ronco C., Ponza R., Benini E. "Aerodynamic Shape Optimization in Aeronautics. A Fast and Effective Multi-Objective Approach", Archives of Computational Methods in Engineering, Vol. 21, 8 August 2014, pp. 189-271, doi: 10.1007/s11831-014-9123-y
10. Massaro A., Benini E., "A Surrogate-Assisted Evolutionary Algorithm Based on the Genetic Diversity Objective", Applied Soft Computing Journal, Vol. 36, November 2015, pp. 87-100 doi: 10.1016/j.asoc.2015.06.026
11. Benini E., Venturelli G., Łaniewski-Wołłk Ł. "Comparison Between Pure and Surrogate-Assisted Evolutionary Algorithms for Multiobjective Optimization", Fuzzy Systems and Data Mining, Vol. 281, 2016, pp. 229-242 doi: 10.3233/978-1-61499-619-4-229

Presented at 47th European Rotorcraft Forum, United Kingdom, 7-9th September, 2021